

This article was downloaded by:

On: 26 January 2011

Access details: *Access Details: Free Access*

Publisher *Taylor & Francis*

Informa Ltd Registered in England and Wales Registered Number: 1072954 Registered office: Mortimer House, 37-41 Mortimer Street, London W1T 3JH, UK



## Nucleosides, Nucleotides and Nucleic Acids

Publication details, including instructions for authors and subscription information:

<http://www.informaworld.com/smpp/title~content=t713597286>

### NMR SOLUTION STRUCTURE AND CONFORMATIONAL ANALYSIS OF THE CALCIUM RELEASE AGENT CYCLIC ADENOSINE 5'-DIPHOSPHATE RIBOSE (cADPR)

Steven M. Graham<sup>a</sup>; Sarah C. Pope<sup>b</sup>

<sup>a</sup> Department of Chemistry, St. John's University, Jamaica, NY, U.S.A. <sup>b</sup> National Institute of Drug Abuse, Baltimore, MD, U.S.A.

Online publication date: 28 February 2001

**To cite this Article** Graham, Steven M. and Pope, Sarah C.(2001) 'NMR SOLUTION STRUCTURE AND CONFORMATIONAL ANALYSIS OF THE CALCIUM RELEASE AGENT CYCLIC ADENOSINE 5'-DIPHOSPHATE RIBOSE (cADPR)', *Nucleosides, Nucleotides and Nucleic Acids*, 20: 3, 169 — 183

**To link to this Article:** DOI: 10.1081/NCN-100002079

**URL:** <http://dx.doi.org/10.1081/NCN-100002079>

PLEASE SCROLL DOWN FOR ARTICLE

Full terms and conditions of use: <http://www.informaworld.com/terms-and-conditions-of-access.pdf>

This article may be used for research, teaching and private study purposes. Any substantial or systematic reproduction, re-distribution, re-selling, loan or sub-licensing, systematic supply or distribution in any form to anyone is expressly forbidden.

The publisher does not give any warranty express or implied or make any representation that the contents will be complete or accurate or up to date. The accuracy of any instructions, formulae and drug doses should be independently verified with primary sources. The publisher shall not be liable for any loss, actions, claims, proceedings, demand or costs or damages whatsoever or howsoever caused arising directly or indirectly in connection with or arising out of the use of this material.

## NMR SOLUTION STRUCTURE AND CONFORMATIONAL ANALYSIS OF THE CALCIUM RELEASE AGENT CYCLIC ADENOSINE 5'-DIPHOSPHATE RIBOSE (cADPR)

Steven M. Graham<sup>1</sup> and Sarah C. Pope<sup>2,\*</sup>

<sup>1</sup>Department of Chemistry, St. John's University, 8000 Utopia Parkway,  
Jamaica, NY 11439

<sup>2</sup>Department of Chemistry, Oklahoma State University,  
Stillwater, OK 74078

### ABSTRACT

A high-resolution NMR study of the solution structure of the calcium release agent cADPR has been performed. Pseudorotationals analysis reveals that in solution both sugar rings in cADPR adopt predominantly (~75%) South conformations, with the A and N rings adopting approximately <sup>2</sup>T<sub>3</sub> (C2'-endo(major)-C3'-exo(minor) and <sup>4</sup><sub>3</sub>T (C3'-exo-C4'-endo) conformations, respectively. The backbone torsion angles  $\beta$  and  $\gamma$  have also been determined. While the minor North conformers were not observed in the crystal structure of cADPR, the solution values of the major South conformers compare well to those found in crystal structure.

### INTRODUCTION

Cyclic adenosine 5'-diphosphate ribose (cADPR) (1), along with nicotinate adenine dinucleotide phosphate (NAADP) (2) and inositol 1,4,5-trisphosphate (IP<sub>3</sub>) (3) are known to cause calcium release from intracellular stores *in vivo*. Each of these molecules is formed as part of a signal cascade initiated by binding of an extracellular signal to a cell surface receptor. A feature shared by these small (molecular weight <750) organic molecules is they are all highly phosphorylated,

---

\*Current address: National Institute of Drug Abuse, 5500 Nathan Shock Dr., Baltimore, MD 21224.

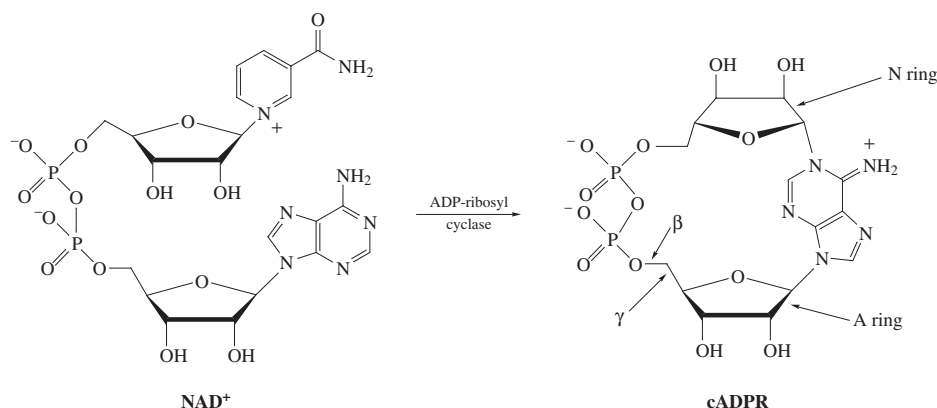


Figure 1.

suggesting that as a class low molecular weight polyphosphates may be important regulators of cellular function.

In biological systems, cADPR is formed from nicotinamide adenine dinucleotide (NAD) by the action of ADP ribosyl cyclase (Figure 1). The cyclase catalyzes a reaction whose end result is the loss of nicotinamide and formation of a new glycosyl bond between adenine and the ribose ring that formerly contained the nicotinamide moiety (the "N ring", Figure 1). In the initial studies (4,5) the exact nature of the new glycosyl bond was unclear, but UV spectroscopy (6) and x-ray crystallography (7) later established that the linkage was from the adenine-N<sub>1</sub> to the N ring C<sub>1'</sub> and that this bond had the  $\beta$ -configuration. The cyclase has a reasonably broad substrate specificity, and has been used to prepare cADPR analogs such as the corresponding cyclic triphosphates, along with analogs containing modified purine and/or ribose rings (8,9). As the number of cADPR analogs grew, we began to ask the question: is it possible to correlate the *solution structure* of these compounds with their *activity*? A logical starting point is then the determination of the solution structure of cADPR using NMR spectroscopy. In general, the literature NMR data for cADPR is of a quality insufficient for detailed structural analysis. One exception is an earlier report by Sekine (10), where it was found that lower temperature spectra (13°C versus room temperature) were of much higher quality. We had independently come to a similar conclusion. We then set out to improve the quality of the spectrum to the point that certain ambiguities in the earlier work regarding the ribose conformations could be resolved, and herein we report the results of our combined multi-pronged NMR and conformational analysis study.

## RESULTS AND DISCUSSION

### 1D and VT Studies

The 1D <sup>1</sup>H NMR spectrum of cADPR in D<sub>2</sub>O at several temperatures is shown in Figure 2. It was immediately apparent that the "room temperature" (27°C)

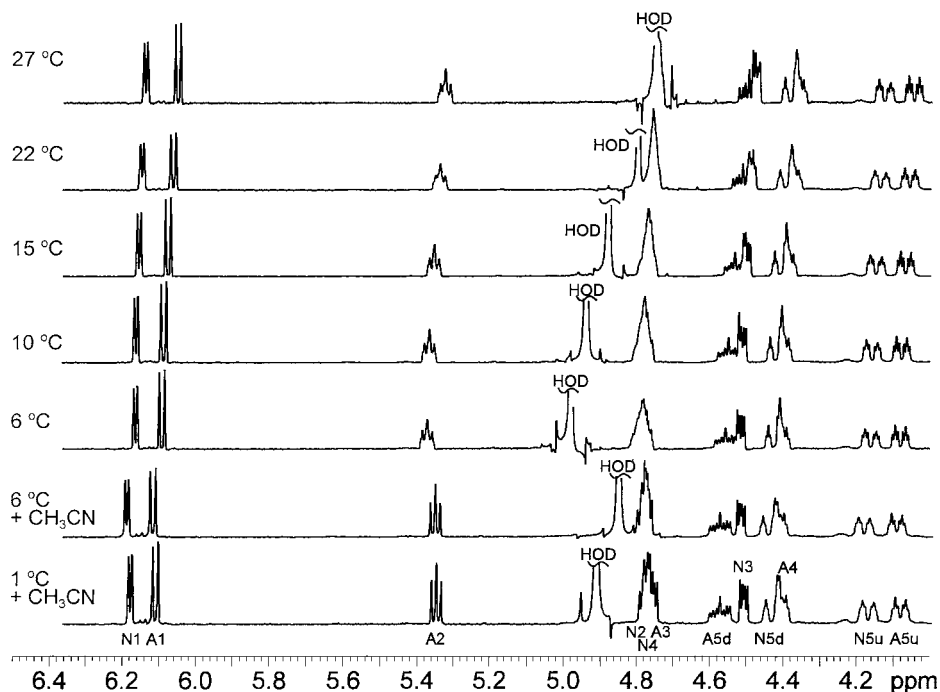


**Figure 2.** 400 MHz VT  $^1\text{H}$  NMR spectra of the sugar ring portion of cADPR in  $\text{D}_2\text{O}$  and  $\text{D}_2\text{O}/\text{CD}_3\text{CN}$ . Assignments were made using COSY.

spectrum would be unsuitable for assignment of the sugar signals and subsequent conformational analysis. Most noticeable was the absence of three of the carbohydrate signals (14 non-exchangeable signals expected versus 11 observed by integration), but equally problematic was the lack of fine detail, needed to extract coupling constants, in the multiplet centered at approximately 4.35 ppm. As previously established (10), the missing signals were obscured by the residual HOD signal, and we undertook variable temperature (VT) experiments in an attempt to shift the position of the HOD signal. After gradually lowering the temperature to 6°C two significant improvements were noticed. First, the HOD signal shifted downfield by approximately 0.2 ppm, which led to the appearance of an ill-defined three-proton multiplet at 4.8 ppm. Second, the two-proton multiplet centered at ~4.5 ppm (27°C) became more dispersed, evolving into two separate, well-defined multiplets at 6°C.

In order to lower the temperature further, and to presumably continue the improvement of the appearance of the spectrum, an NMR solvent titration was performed. Addition of  $\text{CD}_3\text{CN}$  and continued lowering of the temperature produced further improvements, with the best results (bottom spectrum, Figure 2) obtained using an approximate 5:2 v/v mixture of  $\text{D}_2\text{O}/\text{CD}_3\text{CN}$  at 1°C. The improvement is significant in that now all signals are at least well enough resolved to proceed to the next step of the structure assignment process, namely assignment of the sugar  $^1\text{H}$  signals using COSY.

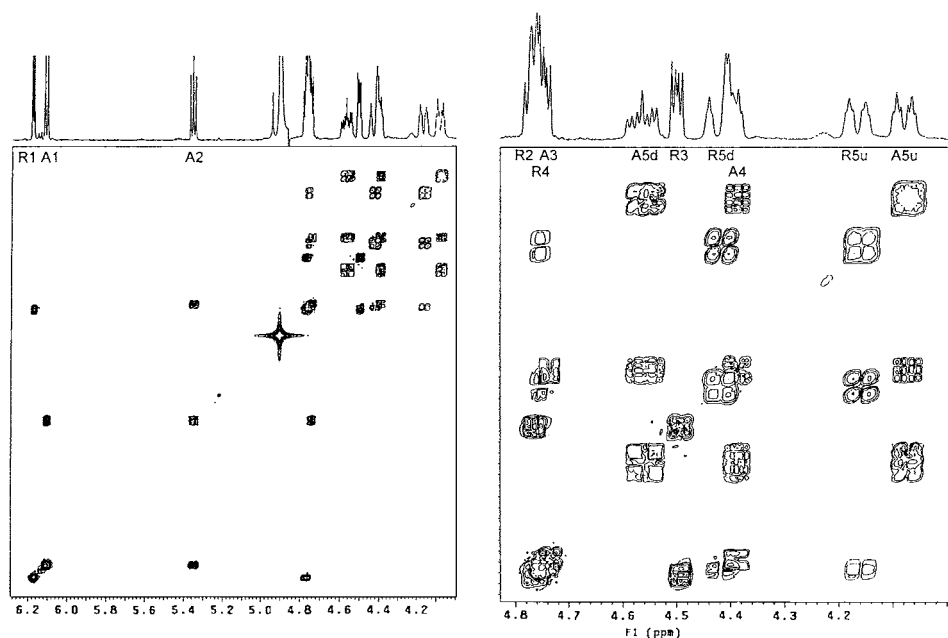


**Figure 3.** 400 MHz COSY spectra (1°C) of the sugar ring portion of cADPR in 5:2 D<sub>2</sub>O:CD<sub>3</sub>CN.

### COSY Assignments

The COSY spectrum of the D<sub>2</sub>O/CD<sub>3</sub>CN/1°C sample of cADPR is shown in Figure 3. The assignment of sugar signals in <sup>1</sup>H NMR is greatly aided by the observation that the anomeric signals (H<sub>1'</sub>) are usually the most downfield aliphatic signals and/or that the diastereotopic methylene signals (H<sub>5'</sub>, H<sub>5''</sub> in riboses) are the most upfield. Given sufficient resolution, each ribose ring of cADPR (A or N, Figure 1) should show six cross peaks: H<sub>1'</sub>–H<sub>2'</sub>, H<sub>2'</sub>–H<sub>3'</sub>, H<sub>3'</sub>–H<sub>4'</sub>, H<sub>4'</sub>–H<sub>5'</sub>, H<sub>4'</sub>–H<sub>5''</sub>, and H<sub>5'</sub>–H<sub>5''</sub> (11).

Our assignments, which are summarized in Table 1, are as follows: Of the downfield sugar signals, the ~6.18 ppm signal was assigned to H<sub>N1'</sub> (i.e., the H<sub>1'</sub> of the N ring) and the ~6.11 ppm signal to H<sub>A1'</sub> (5,10). The H<sub>A1'</sub> signal correlates to the H<sub>A2'</sub> signal at ~5.36 ppm; as H<sub>A2'</sub> is an apparent triplet in the 1D spectrum,  $J_{A1',A2'} \sim J_{A2',A3'}$ . Expansion of the COSY spectrum reveals that H<sub>A2'</sub> correlates with the upfield portion of the three-proton multiplet at 4.80–4.70 ppm, thus revealing H<sub>A3'</sub>. The H<sub>A3'</sub> signal leads to H<sub>A4'</sub>, which is the upfield portion of the two-proton multiplet at ~4.40 ppm. Finally, H<sub>A4'</sub> shows cross peaks to both the upfield (12) (H<sub>A5u</sub>, ~4.08 ppm) and downfield (H<sub>A5d</sub>, the seven peak pattern at ~4.57 ppm) signals of the A ring methylene group. The N ring analysis is complicated slightly by the near chemical shift coincidence of H<sub>N2'</sub> and H<sub>N4'</sub>. Whereas Sekine (10) had found H<sub>N2'</sub> and H<sub>N4'</sub> to be chemical shift coincident (D<sub>2</sub>O, 13°C), our D<sub>2</sub>O/CD<sub>3</sub>CN/1°C sample of cADPR had H<sub>N2'</sub> and H<sub>N4'</sub> at least partially resolved ( $\Delta\delta = 0.013$  ppm, or 5.2 Hz at 400 MHz). Careful analysis of the expanded COSY spectrum (Figure 3)



**Table 1.** Chemical Shift Assignments ( $\delta$ , in ppm)<sup>a</sup>

	A Ring		N Ring	
	This work	Ref. 10	This work	Ref. 10
H <sub>1'</sub>	6.11	6.08	6.18	6.14
H <sub>2'</sub>	5.36	5.36	4.77	4.74
H <sub>3'</sub>	4.75	4.76	4.50	4.49
H <sub>4'</sub>	4.40	4.38	4.76	4.73
H <sub>5d</sub>	4.57	4.53	4.43	4.41
H <sub>5u</sub>	4.08	4.07	4.17	4.15
Other:				
	Ado H2	Ado H8	<sup>31</sup> P	
This work	9.08	8.45	−10.4 (d, $J = 14$ Hz)	
			−11.7 (d, $J = 14$ Hz)	
Ref. 10	8.97	8.38	−9.92 (d, $J = -14.5$ Hz)	
			−10.67 (d, $J = -14.5$ Hz)	

<sup>a</sup> See Figures 2 and 3.

reveals that H<sub>N1'</sub> correlates to the downfield portion of the three-proton multiplet at 4.80–4.70 ppm and that H<sub>N5u</sub> and H<sub>N5d</sub> correlate to the central portion of this multiplet.

### Coupling Constants and Conformational Analysis

With a relatively well-resolved, assigned spectrum of cADPR in hand we were in position to extract the coupling constants needed for conformational analysis of the sugar rings and determination of the conformational equilibrium constants. The relationship between the observed coupling constants in sugar rings and the torsion angles required to produce these coupling constants has been elegantly described using the concept of pseudorotation (13,14). In this treatment, the conformation of a sugar is described in terms of a phase angle,  $P$  (a location on the pseudorotation wheel) and a sugar puckering amplitude,  $\Phi_m$ . A two-state model is assumed (*vide infra*), from which it follows that a particular observed coupling constant is the weighted average of the respective coupling constants of the two rapidly equilibrating conformations. Analysis of a large number of nucleosides and nucleotides has shown that the majority of furanose rings adopt sugar puckers in the “North” (N,  $P \sim 0^\circ$ , C2'-exo-C3'-endo, or  $^3_2T$ )<sup>15</sup> or “South” (S,  $P \sim 180^\circ$ , C2'-endo-C3'-exo, or  $^2_3T$ ) domains of the pseudorotation wheel (Figure 4). Statistically, the North domain centers about  $P_N \sim 9^\circ$  and the South domain about  $P_S \sim 162^\circ$  (13,14). The relationship between the observed coupling constants and the conformational equilibrium is described by Equation 1:

$$J_{a,b \text{ (obs)}} = J_{a,b \text{ (N)}}X_N + J_{a,b \text{ (S)}}X_S \quad (1)$$



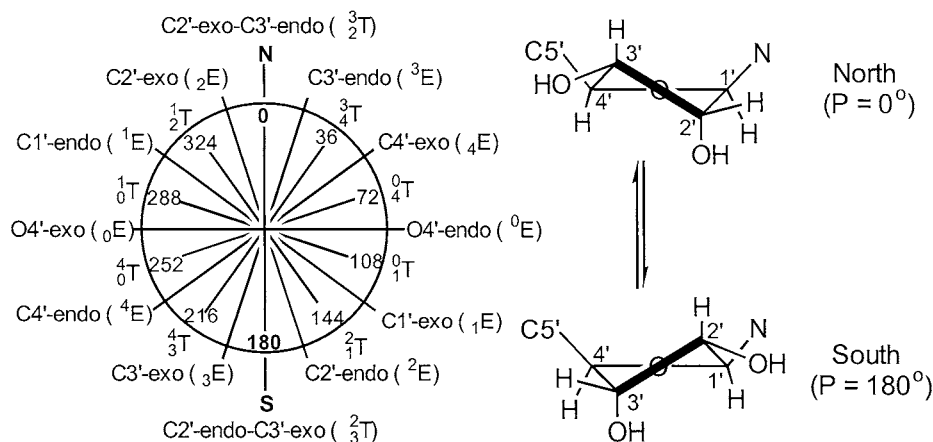


Figure 4.

where  $J_{a,b}(N)$  and  $J_{a,b}(S)$  are the particular coupling constants of the pure N and S conformers and  $X_N$  and  $X_S$  are the mole fractions of the N and S conformers. Given enough coupling constants, whose magnitudes are related to the furanose torsion angles, in principle one can calculate what equilibrium mixture of which two sugar puckers will lead to the observed coupling constants (16). The observed and simulated coupling constants for the A and N rings of cADPR ( $D_2O/CD_3CN/1^\circ C$ ) are summarized in Table 2. Briefly, the procedure was as follows: The  $H_{N1'}$ ,  $H_{N3'}$ , and  $H_{N5u}$  signals were well resolved, and they provide enough information at least *estimate* all but one of the N ring coupling constants. Inspection of the  $H_{N1'}$  doublet reveals  $J_{N1',N2'} \sim 3.7$  Hz.  $H_{N3'}$  is a doublet of doublets ( $J = 4.9, 2.9$  Hz), giving the magnitude, but not the absolute assignments, of  $J_{N2',N3'}$  and  $J_{N3',N4'}$ .  $H_{N5u}$  is an apparent doublet of broad triplets, with a large  $^2J_{N5u,N5d}$  of  $\sim 12$  Hz; the “triplet” portion of this signal is caused by the nearly similar values (2–3 Hz) of  $J_{N4',N5u}$  and  $^3J_{N5u-C5'-O5'-P}$ . A similar treatment of the A ring coupling constants allowed estimation of all the coupling constants except  $J_{A3',A4'}$ . Next, spectral simulation was used to further refine the extracted coupling constants (17). The observed and simulated spectra are shown in Figure 5 (rms error = 0.2 Hz) and the chemical shift and coupling constant data are summarized in Table 1 and Table 2.

With the cADPR coupling constants now established, we turned our attention to the pseudorotational analysis—converting the coupling constants into descriptions of the ribose ring conformations. First, the decision was made to avoid using the simplifying approximation that the South-to-North ratio can be obtained from the ratio of  $J_{1'2'}$  and  $J_{3'4'}$  ( $S/N = J_{1'2'}/J_{3'4'}$ ). Due to the novel, cyclic structure of cADPR, it seemed reasonable to expect that the A and N ribose rings might adopt geometries substantially different from the “typical” (18) values ( $P_N \sim 9^\circ$  and  $P_S \sim 162^\circ$ ) found in many nucleos(t)ides—and it is precisely these typical values from which the  $S/N = J_{1'2'}/J_{3'4'}$  rule was derived (13,18). In other words, use of the  $S/N = J_{1'2'}/J_{3'4'}$  rule *assumes* ribose conformations at or near values of

## NMR STRUCTURE OF cADPR

175

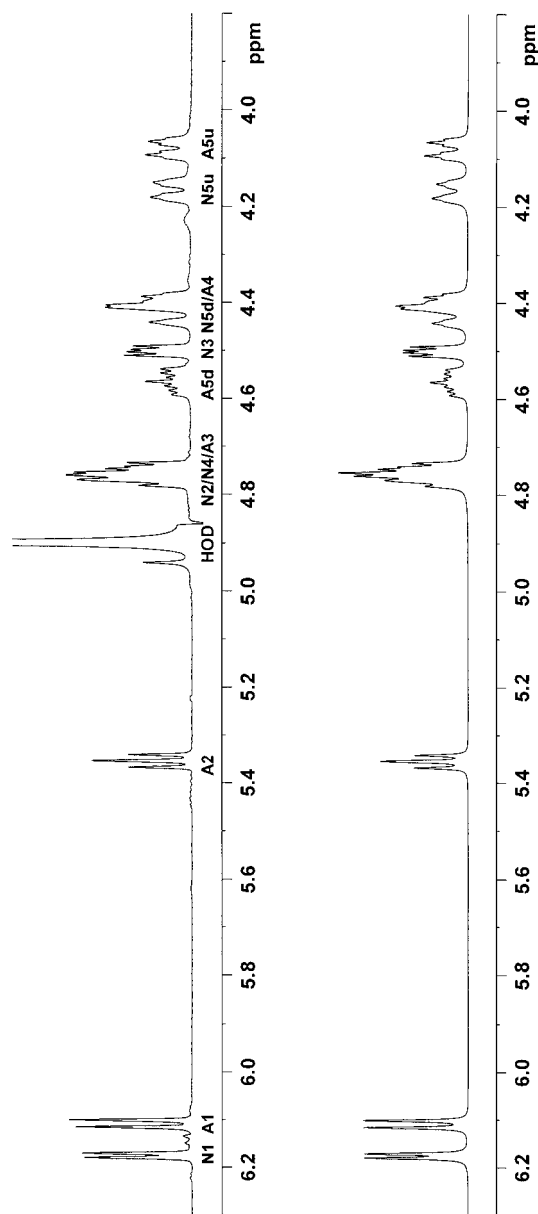


**Figure 5.** 400 MHz  $^1\text{H}$  NMR spectrum of the sugar ring portion of cADPR for the  $1^\circ$   $\text{C D}_2\text{O/CD}_3\text{CN}$  sample (upper) and the simulated spectrum (lower).



**Table 2.** Observed and Simulated Coupling Constants ( $J$ , in Hz)

	A Ring			N Ring		
	Observed <sup>a</sup>	Simulated	Ref. 10	Observed	Simulated	Ref. 10
$J_{1'2'}$	$5.6 \pm 0.2$ (3) <sup>b</sup>	5.9	5.6	3.7 (1)	3.6	3.7
$J_{2'3'}$	$5.2 \pm 0.2$ (4)	5.0	5.1	$4.9 \pm 0.1$ (2)	4.9	5.1
$J_{3'4'}$	$2.8 \pm 0.2$ (4)	3.0	3.2	$2.9 \pm 0.1$ (2)	2.8	2.7
$J_{4'5u'}$	$2.8 \pm 0.3$ (5)	2.6	2.6	2–3 <sup>c</sup>	2.9	2.2
$J_{4'5d'}$	$7.2 \pm 0.2$ (6)	7.2	6.8	2–3 <sup>c</sup>	2.6	2.2
$J_{5u'5d'}$	$-10.9 \pm 0.2$ (6)	-11.0	-11.0	$-12.0 \pm 0.1$ (2)	-11.9	-11.9
$J_{p'5u'}$	$2.9 \pm 0.2$ (3)	3.0	3.4	2–3 <sup>c</sup>	2.9	3.7
$J_{p'5d'}$	$3.5 \pm 0.2$ (4)	3.5	3.9	2–3 <sup>c</sup>	2.6	2.2

<sup>a</sup> Observed  $\pm$  average deviation.

<sup>b</sup> Number of measurements.

<sup>c</sup> Value estimated from the half-height linewidth; confirmed by simulation.

$P_N \sim 9^\circ$  and  $P_S \sim 162^\circ$ , and only when this assumption is justified can the rule be used to estimate the  $N \rightleftharpoons S$  equilibrium reliably. Because of this limitation that we used Altona's method (13) to explore wide *ranges* of conformations in the North and South pseudorotational domains.

A summary of the procedure used is as follows: The Altona values (13) of  $J_{1'2'}$ ,  $J_{2'3'}$ , and  $J_{3'4'}$  calculated for conformationally pure nucleos(t)ide ribose rings were used to calculate the time-averaged coupling constants one would observe as  $P_N$ ,  $P_S$ , and the N:S ratio were systematically varied. We then sought the best fit of these calculated coupling constants to the coupling constants extracted from the simulated cADPR spectrum. For a given ratio of N and S conformers a good fit was defined as one where **each** calculated  $J$  was within  $\pm 0.3$  Hz of the value determined by simulation. The results are summarized in Table 3. For each ribose ring of cADPR we explored combinations of  $P_N = 342^\circ - 36^\circ$  and  $P_S = 144^\circ - 234^\circ$ , using puckering amplitudes of  $\Phi_m = 35^\circ$  and  $40^\circ$  (16). One of the significant findings (*vide infra*) was that in solution both the A and N rings of cADPR each contained  $\sim 25\%$  of the North conformer – neither of which was observed in the crystal structure (7) – and that the N ribose ring  $P_S$  was shifted to an atypically high value of  $\sim 216^\circ$ .

For the A ring eight pairs of N/S conformers were found (Table 3, Entries 1–8). The fit of the calculated versus simulated coupling constants, expressed as the rms error, was quite good, ranging from 0.12–0.21 Hz. The coupling constants for the A ring ( $\Phi_m = 35^\circ$ ) are consistent with an N:S ratio of 25:75 for  $P_N$  values of  $351^\circ - 27^\circ$  ( ${}^2T^3 - {}^3T_4$ ) and  $P_S$  values of  $162^\circ - 180^\circ$  ( ${}^2E - {}^2_3T$ ). When the A ring  $\Phi_m$  was increased to  $40^\circ$  all of the previous N:S populations were now excluded. Recovery of N:S populations for  $\Phi_m = 40^\circ$  was possible if the  $\Delta J$  fit criterion was relaxed from  $\pm 0.3$  Hz to  $\pm 0.4$  Hz (not shown). Under this relaxed fit criterion, the N:S populations were essentially unchanged (70–75% S) although  $P_N$  and  $P_S$  occupied slightly wider ranges ( $P_N = 342^\circ - 36^\circ$  and  $P_S = 162^\circ - 189^\circ$ ) and the average rms



## NMR STRUCTURE OF cADPR

177

**Table 3.** Comparison of Coupling Constants Calculated for Various N:S Populations of a Ribose Ring (13) to Those Extracted from Simulation of the D<sub>2</sub>O/CD<sub>3</sub>CN/1°C Spectrum of cADPR

	Entry	$\Phi_m$	$P_N, P_S$	%S:%N	Calculated $J$ 's			rms <sup>b</sup>
					$J_{1/2'}$	$J_{2/3'}$	$J_{3/4'}$	
<b>A Ring</b>			<b>SIMULATED</b>		<b>5.90</b>	<b>5.00</b>	<b>3.00</b>	
	1	35°	351, 162	75:25	5.92	5.27	2.88	0.17
	2	35°	0, 162	75:25	5.92	5.25	3.00	0.15
	3	35°	9, 162	75:25	5.94	5.27	3.08	0.16
	4	35°	0, 171	75:25	5.75	5.12	2.79	0.16
	5	35°	9, 171	75:25	5.77	5.13	2.88	0.13
	6	35°	18, 171	75:25	5.81	5.18	2.94	0.12
	7	35°	27, 171	75:25	5.88	5.25	2.97	0.15
	8	35°	27, 180	75:25	5.63	5.21	2.85	0.21
	9	40°	None found <sup>c</sup>					
<b>N Ring</b>	<b>Averages, Entries 1–8:</b>		<b>10,169</b>	<b>75:25</b>	<b>5.83</b>	<b>5.21</b>	<b>2.92</b>	<b>0.16</b>
	From Ref. 10:	35°	9, 162	64:36	5.35	5.25	3.73	0.35
	From Ref. 10:	40°	9, 162	64:36	5.62	4.57	3.75	0.44
		<b>SIMULATED</b>			<b>3.60</b>	<b>4.90</b>	<b>2.80</b>	
	12	35°	None found					
	13	40°	351, 216	70:30	3.72	5.14	3.05	0.21
	14	40°	0, 216	75:25	3.89	5.17	2.81	0.23
	15	40°	9, 216	75:25	3.89	5.19	2.89	0.24
	<b>Averages, Entries 13–15:</b>		<b>0,216</b>	<b>73:27</b>	<b>3.83</b>	<b>5.16</b>	<b>2.91</b>	<b>0.23</b>
	From Ref. 10:	35°	9, 162	59:41	4.90	5.23	4.23	1.13
	From Ref. 10:	40°	9, 162	59:41	5.13	4.55	4.30	1.28

<sup>a</sup>Only N:S ratios that produced all calculated  $J$ 's within  $\pm 0.3$  Hz of the values determined by simulation are shown.

<sup>b</sup>Rms error in Hz, calculated vs. simulated (this work) or calculated vs. observed (Ref. 10) coupling constants.

<sup>c</sup>No good fit could be found with this value of  $\Phi_m$ ; see text.

error increased to 0.27 Hz. Analysis of the N ring revealed an opposite trend – no good fit with  $\Phi_m = 35^\circ$ , whereas with  $\Phi_m = 40^\circ$  three pairs of N/S conformers were found (Table 3, Entries 13–15). The N:S ratios ranged from 30:70 to 25:75, with  $P_N$  spanning the range from  $351^\circ\text{--}9^\circ$  ( ${}^2T^3/{}^3T_2$ ). Interestingly, the N ring  $P_S$  localized to  $216^\circ$  ( ${}^4T$ ). The average rms error for these three N:S pairs was 0.23 Hz. No populations of N:S conformers could be found for  $\Phi_m = 35^\circ$  until the  $\Delta J$  fit criterion was relaxed to  $\pm 0.5$  Hz, and even this loosening of the fit revealed only a single N:S pair (N:S = 40:60,  $P_N = 342^\circ$ ,  $P_S = 198^\circ$ ) with a very large rms error of 1.12 Hz. In the published crystal structure of cADPR (7) the A ring was found to adopt a C2'-endo (major)-C3'-exo (minor) conformation ( $P_S \sim 171^\circ$ ,  ${}^2T_3$ ); the N ring conformation was stated to be C3'-exo ( $P_S \sim 198^\circ$ ,  ${}^3E$ ) with a C4'-O4'-C1'-C2' torsion angle of  $+6^\circ$ , which is probably better described as C3'-exo-C4'-endo ( $P_S \sim 216^\circ$ ,  ${}^4T$ ). Limiting our attention to the major solution conformers of the A and N rings ( $P_S = 162\text{--}180^\circ$  and  $216^\circ$ , respectively), we find the agreement between the crystal structure and our solution structure, at the current level of sophistication, to be quite good (19).

It is instructive to compare our pseudorotation parameters for the N ring of cADPR ( $P_N = 351^\circ\text{--}9^\circ$ ,  $P_S = 216^\circ$ ,  $\Phi_m = 40^\circ$ , N:S = 25:75) to those obtained by Sekine (10), who suggested that the N ring exists either as a 41:59 N:S mixture or that it exists in an undefined “flat” conformation. The Sekine proposal of a 41:59 N:S mixture for the N ring of cADPR is unlikely, for two reasons. First, the 41:59 N:S mixture was estimated using the  $S/N = J_{1'2'}/J_{3'4'}$  rule (18). As discussed above, this rule is based on the assumption that  $P_N$  and  $P_S$  are at or near the statistical average values ( $9^\circ$  and  $162^\circ$ , respectively). Using Sekine's N ring ribose coupling constants with  $P_N = 9^\circ$ ,  $P_S = 162^\circ$ , and N:S = 41:69, we calculate ribose ring coupling constants with rms errors in excess of 1 Hz (Table 3, Entries 16, 17). Once  $P_N$  and  $P_S$  diverge from the average values  $J_{1'2'}$  and  $J_{3'4'}$  will change, and thus so will the S/N ratio. Second, our pseudorotational analysis revealed only one case where the N:S ratio was  $\sim 40:60$  (*vide supra*), albeit under the relaxed fit criterion of  $\Delta J = \pm 0.5$  Hz and with a poor rms fit of 1.12 Hz.

The alternative proposal that the N ring of cADPR is “flat” is also unlikely. It is well established that flattened ribose rings (small  $\Phi_m$ ) will show large values of  $J_{2'3'}$  and small values of the sum  $J_{1'2'} + J_{3'4'}$ . Small  $\Phi_m$ , large  $J_{2'3'}$ , and small  $J_{1'2'} + J_{3'4'}$  are generally taken to mean smaller than  $35^\circ$ , larger than 5.2 Hz, and smaller than  $\sim 9$  Hz, respectively (13,18). While the N ring of cADPR meets the last criterion ( $J_{1'2'} + J_{3'4'} = 6.4$  Hz), the value of the N ring  $J_{2'3'}$  (4.9 Hz) is well within the range of normally puckered riboses for  $P_N = 0 \pm 18^\circ$  and  $P_S = 180 \pm 18^\circ$  of any N:S ratio. The observation that the sum  $J_{1'2'} + J_{3'4'}$  is significantly different from  $\sim 9$  Hz does not *by itself indicate an abnormally puckered ribose*; changes in  $J_{2'3'}$  are also required. Indeed, deviations in the sum  $J_{1'2'} + J_{3'4'}$  are usually attributed to shifts of  $P_N$  to values lower than  $\sim 9^\circ$  and/or  $P_S$  to values higher than  $\sim 162^\circ$ . This is exactly the trend suggested by our pseudorotational analysis.



In fact, our data indicate that the cADPR N ring is slightly *more* puckered ( $\Phi_m = 40^\circ$ ) than usual, not substantially *less*. Further evidence can be obtained from a more detailed analysis of  $J_{2'3'}$ , as this coupling constant is highly sensitive to changes in  $\Phi_m$ . For a ribose of constant phase angle  $P$ ,  $J_{2'3'}$  always *increases* with decreasing  $\Phi_m$  (increased flattening), except in the typically “disallowed” regions of  $P \sim 90^\circ$  and  $270^\circ$ . For every  $5^\circ$  decrease in  $\Phi_m$ ,  $J_{2'3'}$  increases by 0.55–0.72 Hz for  $P_N = 0 \pm 36^\circ$  and  $P_S = 180 \pm 36^\circ$  (13). This analysis thus predicts that even a modest flattening of the N ring ribose to  $\Phi_m = 30^\circ$  and a North population as high as 50% would yield a  $J_{2'3'}$  of *at least*  $\sim 5.8$  Hz for any combination of  $P_N = 0 \pm 36^\circ$  and  $P_S = 180 \pm 36^\circ$ . As  $P_S$  tends towards the upper end of this range, the calculated  $J_{2'3'}$  becomes even larger. Using our values from the N ring our pseudorotational analysis (average  $P_N = 0^\circ$ ,  $P_S = 216^\circ$ , N:S = 25:75), we calculate an N ring  $J_{2'3'}$  of  $\sim 6.3$  Hz for  $\Phi_m = 30^\circ$ , which is substantially different than the observed value of 4.9 Hz.

The Sekine proposal of a flat N ring is based (1) their interpretation of the cADPR crystal structure, an interpretation which is almost certainly incorrect, and (2) their own ROESY data, for which alternate explanations are possible. In the cADPR crystal structure the N ring conformation was stated to be C3'-exo ( $P_S \sim 198^\circ$ ,  $^3E$ ), not flat, as Sekine says. An ideal  $^3E$  would have an endocyclic torsion angle C4'-O4'-C1'-C2' ( $\nu_o$ ) of  $0^\circ$ ; the observed  $\nu_o$  torsion angle was  $+6^\circ$ , which shifts the conformation to  $P_S \sim 216^\circ$  ( $^4T$ ). A *single* endocyclic torsion angle near  $0^\circ$  is not evidence for a flat conformation (20). Further evidence for a flat N ring was the observation of weak ROESY cross peaks from the adenine ring H2 to  $H_{N2'}$  and  $H_{N3'}$ , and the supposition that the  $A_{H2}-H_{N3'}$  distance in a  $^2E$  conformation and the  $A_{H2}-H_{N2'}$  distance in a  $^3E$  conformation is “too long” to observe an ROE. Implicit in this argument is the presence of only one conformer ( $^2E$  or  $^3E$ ) and that the N ring glycosidic torsion angle remains constant during  $N \rightleftharpoons S$  transitions. pseudorotational analysis clearly shows an  $N \rightleftharpoons S$  equilibrium, and the constrained nature of the cADPR macrocycle suggests that changes in ribose pucker will be transmitted to the glycosidic torsion angle. In our view, an N ring N:S ratio of 25:75 and a  $P_S$  of  $\sim 216^\circ$  ( $^4T$ ) can easily accommodate the ROESY cross peak intensities, and so neither the assertion that the N ring N:S ratio is  $\sim 40:60$  (for *any*  $P_N$  and  $P_S$ ) or that the N ring is unusually flat can be justified.

The observation of moderate populations of the North conformer in solution (and their absence in the crystal structure) raises an intriguing question: What is the biologically active conformation of cADPR? In the limiting case where one considers only the  $N \rightleftharpoons S$  equilibria of the A and N rings there are four possible structures, i.e., both rings could be S ( $A_S N_S$ ), one could be S and the other N ( $A_S N_N$  or  $A_N N_S$ ), or both could be N ( $A_N N_N$ ). Using our 25:75 N:S ratios for each ring predicts an  $A_S N_S : A_S N_N : A_N N_S : A_N N_N$  ratio of 56:19:19:6, any one of which could be the active conformer. Our solution data suggest that to a first approximation almost half (44%) of the molecules in solution *do not adopt the conformation found in the crystal structure*, demonstrating again that NMR solution data can be



a valuable and necessary supplement to crystal structure data. This distribution is also based on the assumption that a conformational change in one ring does not *induce* a change in the other. We have not begun to address the relative energies of the various solution conformers, and additional studies with cADPR and analogs will be required before this idea can be pursued.

The coupling constant data has also been used to determine the backbone torsion angles  $\beta$  (P-O5'-C5'-C4' via the  $^3J_{\text{P-H5'}/5''}$  coupling) (21) and  $\gamma$  (O5'-C5'-C4'-C3' via the  $^3J_{\text{H4'}-\text{H5'}/5''}$  coupling) (22,23). For the A ring the coupling of the phosphorus to both H<sub>A5u</sub> and H<sub>A5d</sub> is quite similar (3.0 and 3.5 Hz, respectively), suggesting a symmetrical relationship. Reasonably assuming a staggered conformation about the  $\beta$ -bond leads to the conclusion that the phosphorus is *gauche* to both H<sub>5'</sub> and H<sub>5''</sub>, and thus *trans* to C4'. Analogous behavior was observed for the N ring, and thus both the A and N ring  $\beta$ -bonds are likely to be almost exclusively (> 90%) *trans* (torsion angle =  $\pm 180^\circ$ ). Sekine (10) came to a similar conclusion. The crystal structure  $\beta$ -bonds are in the same general range as our solution values, with an A ring  $\beta$  of  $-138^\circ$  and an N ring  $\beta$  of  $+160^\circ$ . In the case of the N ring  $\gamma$ -bond (22,23) we observed near equivalence of  $J_{\text{N4',N5u}}$  and  $J_{\text{N4',N5d}}$  (2.9 and 2.6 Hz, respectively). Using the same logic as above gives thus places H<sub>N4'</sub> *gauche* to both H<sub>N5u</sub> and H<sub>N5d</sub>, i.e., the N ring C3' and O5' are *gauche* and the N ring  $\gamma$ -bond is (> 80%)  $\gamma^+$  (torsion angle =  $+60^\circ$ ). Using their coupling constant data, Sekine came to a similar conclusion, but their ROESY data led to the proposal that the N ring  $\gamma$ -bond has the  $\gamma^t$  conformation. Given that even small perturbations from the ideal  $\gamma^+$  geometry could produce H<sub>4'</sub>-H<sub>5'</sub> and H<sub>4'</sub>-H<sub>5''</sub> ROESY cross peaks of differing intensity we see no compelling reason to assume an N ring  $\gamma^t$  conformation (24). Analysis of the A ring  $\gamma$ -bond is complicated because we have not yet made the stereospecific assignments of H<sub>A5u</sub> and H<sub>A5d</sub> to H<sub>5'</sub> and/or H<sub>5''</sub> (24,25). In the absence of the stereospecific assignments of H<sub>A5u</sub> and H<sub>A5d</sub> we prefer to interpret a "small"  $J_{\text{A4',A5u}}$  (2.6 Hz) and a "large"  $J_{\text{A4',A5d}}$  (7.2 Hz) coupling as evidence for approximately 35%  $\gamma^+$  and either 65%  $\gamma^t$  ( $\pm 180^\circ$ ) or 65%  $\gamma^-$  ( $-60^\circ$ ) (22-26). The solution values for the N and A ring  $\gamma$ -bonds ( $\gamma^+:\gamma^t \sim 80:20$  and  $\sim 35:65$ , respectively, assuming negligible  $\gamma^-$ ) differ from those found in the crystal structure (both  $\gamma^t$ , with the N ring ( $\gamma = +174^\circ$ ) and the A ring ( $\gamma = -174^\circ$ ) (27). Besides crystal packing forces, another possible explanation is that the x-ray crystal structure was determined on the free acid of cADPR, whereas our solution structure is the potassium salt, and the ionization state of the phosphorus is likely to play a major role in determining at least some of the backbone torsion angles.

In conclusion, we have presented high-resolution NMR data supporting the following solution structure for cADPR: The A ring major conformation is approximately  $^2T_3$  ( $P_S = 171 \pm 9^\circ$ ), the N ring major conformation is approximately  $^4T$  ( $P_S = 216^\circ$ ), both ring  $\beta$ -bonds are *trans*, the N ring  $\gamma$ -bond is  $\gamma^+$ , and the A ring  $\gamma$ -bond is 35%  $\gamma^+$  and either 65%  $\gamma^t$  or  $\gamma^-$ . Further work, especially modeling studies and NOE experiments to stereospecifically assign H<sub>5'</sub> and H<sub>5''</sub>, will be reported in due course.



## EXPERIMENTAL

**Synthesis:** The potassium salt of cADPR was synthesized and purified as described (28), substituting ADP ribosyl cyclase (Sigma) for pig brain acetone powder.

**NMR:**  $^1\text{H}$  (400 MHz) and  $^{31}\text{P}$  (121.5 MHz) NMR spectra were recorded on a Varian INOVA spectrometer. Pure  $\text{D}_2\text{O}$  (> 99.8%) samples were referenced to the residual HOD peak in a temperature-dependent fashion as described (29). Samples run in  $\text{D}_2\text{O}/\text{CD}_3\text{CN}$  were referenced to the previous non- $\text{CD}_3\text{CN}$  containing sample.  $^{31}\text{P}$  NMR spectra were referenced to external 85%  $\text{H}_3\text{PO}_4$  in  $\text{D}_2\text{O}$ . NMR samples were lyophilized three times from  $\text{D}_2\text{O}$  prior to final dissolution in  $\text{D}_2\text{O}$ . 1D NMR spectra were acquired for 2.7 seconds (32 transients) with a 5 second pulse delay, using a spectral width of 6000 Hz, 32K data points, and zero-filled to 64K. No solvent suppression was used and the data was processed with a Gaussian (0.1) and line broadening (−1.0 Hz) weighting functions. The COSY experiment was performed in absolute value mode using 16 transients per increment, 512 increments, with an acquisition time of 1.11 seconds, a 2.0 second delay, a spectral width of 3600 Hz, and zero-filled to  $8\text{K} \times 8\text{K}$  points. After sine bell weighting (0.3 seconds) in both dimensions, the data was symmetrized.  $^1\text{H}$  NMR ( $\text{D}_2\text{O}/\text{CD}_3\text{CN}$ ,  $1^\circ\text{C}$ )  $\delta$  9.08 (s, 1H, adenine H2); 8.45 (s, 1H, adenine H8); 6.18 (d,  $J = 3.7$  Hz, 1H,  $\text{H}_{\text{N}1'}$ ); 6.11 (d,  $J = 5.9$  Hz, 1H,  $\text{H}_{\text{A}1'}$ ); 5.36 (d,  $J = 5.4$  Hz, 1H,  $\text{H}_{\text{A}2'}$ ); 4.77–4.76 (m, 2H,  $\text{H}_{\text{N}2'}$ ,  $\text{H}_{\text{N}4'}$ ); 4.75 (dd,  $J = 5.0, 2.9$  Hz, 1H,  $\text{H}_{\text{A}3'}$ ); 4.57 (ddd,  $J = -10.9, 7.3, 3.5$  Hz, 1H,  $\text{H}_{\text{A}5\text{d}}$ ); 4.50 (dd,  $J = 4.9, 2.9$  Hz, 1H,  $\text{H}_{\text{N}3'}$ ); 4.43 (app dt,  $J = -11.9, \sim 2$  Hz, 1H,  $\text{H}_{\text{N}5\text{d}}$ ); 4.40 (app dt,  $J = 7.0, 2.8$  Hz, 1H,  $\text{H}_{\text{A}4'}$ ); 4.17 (app dt,  $J = -12.1, \sim 3$  Hz, 1H,  $\text{H}_{\text{N}5\text{u}}$ ); 4.08 (dt,  $J = -11.1, 2.9$  Hz, 1H,  $\text{H}_{\text{A}5\text{u}}$ ).  $^{31}\text{P}$  NMR ( $\text{D}_2\text{O}/\text{CD}_3\text{CN}$ )  $\delta$  10.4 (d,  $J = -14$  Hz); 11.7 (d,  $J = -14$  Hz).

## ACKNOWLEDGMENTS

This work was supported by St. John's University and by an NIH grant (GM 54261) to SMG.

## REFERENCES

1. Lee, H.-C. *Physiol. Rev.* **1997**, 77, 1133–1164.
2. Lee, H.-C.; Aarhus, R. *J. Biol. Chem.* **1995**, 270, 2152–2157.
3. Berridge, M.J. *Nature* **1993**, 361, 315–325.
4. Clapper, D.L.; Walseth, T.F.; Dargie, P.J.; Lee, H.C. *J. Biol. Chem.* **1987**, 262, 9561–9568.
5. Lee, H.-C.; Walseth, T.F.; Bratt, G.T.; Hayes, R.N.; Clapper, D.L. *J. Biol. Chem.* **1989**, 264, 1608–1615.
6. Kim, H.; Jacobson, E.L.; Jacobson, M.K. *Biochem. Biophys. Res. Comm.* **1993**, 194, 1143–1147.





7. Lee, H.-C.; Aarhus, R.; Levitt, D. *Nature Struct. Biol.* **1994**, *1*, 143–144.
8. Cyclic triphosphates: Zhang, F.-J.; Sih, C.J. *Bioorg. Med. Chem. Lett.* **1997**, *7*, 1753–1756. Modified purine/ribose rings: Graeff, R.M.; Walseth, T.F.; Hill, H.K.; Lee, N.C. *Biochemistry* **1996**, *35*, 379–386. Walseth, T.F.; Lee, H.C. *Biochim. Biophys. Acta* **1993**, *1178*, 235–242. Ashamu, G.A.; Sethi, J.K.; Galione, A.; Potter, B.V.L. *Biochemistry* **1997**, *36*, 9509–9517. Bailey, V.C.; Sethi, J.K.; Galione, A.; Potter, B.V.L. *J. Chem. Soc., Chem. Comm.* **1997**, 695–696. Ashamu, G.A.; Galione, A.; Potter, B.V.L. *J. Chem. Soc., Chem. Comm.* **1995**, 1359–1360.
9. A non-enzymatic preparation of a carbocyclic derivative has been reported. See Shuto, S.; Shirato, M.; Sumita, Y.; Ueno, Y.; Matsuda, A. *J. Org. Chem.* **1998**, *63*, 1986–1994.
10. Wada, T.; Inageda, K.; Arimoto, K.; Tokita, K.-i.; Nishina, H.; Takahashi, K.; Katada, T.; Sekine, M. *Nucleosides Nucleotides* **1995**, *14*, 1301–1314.
11. All descriptions of nucleos(t)ide conformation herein conform to the IUPAC/IUB Joint Commission on Biochemical Nomenclature guidelines. See *Eur. J. Biochem.* **1983**, *131*, 9.
12. At the current time we have not stereospecifically assigned the  $H_{5'}$  and  $H_{5''}$  protons.
13. de Leeuw, F.A.A.M.; Altona, C. *J. Chem. Soc. Perkin II* **1982**, 375–384.
14. Altona, C.; Sundaralingam, M. *J. Am. Chem. Soc.* **1972**, *94*, 8205–8212.
15. In the E/T symbolism, E denotes an envelope and T a twist conformation. Subscripts and superscripts denote that the indicated atom has the exo or endo configuration, respectively. Symmetrical twist forms have both the subscript and superscript on the same side of the T. For asymmetrical twist conformations, the subscript or superscript before the T denotes the major conformation. For example, the symmetrical twist conformation C2'-endo-C3'-exo ( $P = 180^\circ$ ) would be described as  ${}^2_3T$ , where as the asymmetrical twist conformation, C2'-endo (major)- C3'-exo (minor) ( $P = 171^\circ$ ), would be described as  ${}^2T_3$  (Ref. 11).
16. Two points should be stressed. First, in the full treatment described in the literature,  ${}^3J_{HH}$  is a function of five variables -  $P_N$ ,  $\Phi_N$ ,  $P_S$ ,  $\Phi_S$ , and  $X_N$  (or  $X_S$ , since  $X_N + X_S = 1$ ). Deoxy sugars can be completely determined, as there are five observable values related to the endocyclic torsion angles -  $J_{1'2'}$ ,  $J_{1'2''}$ ,  $J_{2'3'}$ ,  $J_{2''3'}$ , and  $J_{3'4'}$ . Ribo sugars, on the other hand, have only three coupling constants related to the endocyclic torsion angles -  $J_{1'2'}$ ,  $J_{2'3'}$ , and  $J_{3'4'}$ . Ribo sugars are therefore “underdetermined” and assumptions concerning two of the variable must be made. In practice,  ${}^3J_{HH}$  shows relatively little dependence on the puckering amplitude,  $\Phi$  (the variation in  $\Phi$  is typically 1 Hz or less over most of its allowed range). In our study we have constrained  $\Phi$  to two values,  $35^\circ$  and  $40^\circ$ . The second point concerns the dynamic equilibrium between N and S conformers. Strictly speaking, **all** N conformers exist in **one** potential energy well (i.e., there is a *continuum* of N conformers), and all S conformers exist in another. There **is** an energy barrier to N/S interconversion, but the barrier for “interconversions” **between** various N conformers (and likewise, between S conformers) is small or non-existent. See also reference 18.
17. Spectra were simulated using NMRSIM 2.8, a component of XWIN-NMR 2.6 (Bruker Instruments).
18. Altona, C.; Sundaralingam, M. *J. Am. Chem. Soc.* **1973**, *95*, 2333–2344.
19. For the sake of completeness, the glycosidic torsion angles, from reference 7, are: A ring ( $O_4'-C_1'-N_9-C_4$ ) =  $+64^\circ$  (*syn*) and R ring ( $O_4'-C_1'-N_1-C_6$ ) =  $-167^\circ$  (*anti*).
20. All ideal envelope conformations have one endocyclic torsion angle of  $0^\circ$ .



21. Lankhorst, P.P.; Haasnoot, C.A.G.; Erkelens, C.; Altona, C. *J. Biomol. Struct. Dyn.* **1984**, *1*, 1387–1405. This reference provides the “sum rule” estimate for the fraction of  $\beta$  in the *trans* conformation:  $f_{\beta t} = (25.5 - J_{H5'P} - J_{H5''P})/20.5$ .
22. Haasnoot, C.A.G.; de Leeuw, F.A.A.M.; de Leeuw, H.P.M.; Altona, C. *Recl. Trav. Chim. Pays-Bas* **1979**, *98*, 576–577.
23. Provided the population of the  $\gamma^-$  conformation is negligible, as is often assumed, the fraction of the population in the  $\gamma^+$  conformation can be estimated by  $f_{\gamma^+} = [13.3 - (J_{4'5'} + J_{4'5''})]/9.7$ ; the balance is therefore  $\gamma^+$ . If, however, the  $\gamma^-$  population is significant and the  $\gamma^+$  population is negligible, this formula still estimates the fraction of  $\gamma^+$ , but now the balance is  $\gamma^-$ . See Altona, C. *Recl. Trav. Chim. Pays-Bas*, **1982**, *101*, 413–433.
24. There is some question as to the degree of certainty of Sekine's (reference 10)  $H_{5'}$  and  $H_{5''}$  assignments. First, the procedure for the stereospecific assignments was not detailed. It appears to have been based single pairs of ROESY cross peak intensities (e.g., comparison of the  $H_{4'}/H_{5'}$  to the  $H_{4'}/H_{5''}$  cross peak) and in no cases was a confirming pair of cross peaks observed. Second, the  $H_{5'}$  and  $H_{5''}$  labels appear to be reversed, at least according the IUPAC/IUB Joint Commission on Biochemical Nomenclature guidelines (Ref. 11). In fact, the Sekine ROESY data, if interpreted using the IUPAC/IUB JCBN rules, suggests the  $\gamma^-$ , not the  $\gamma^+$  conformation for the R ring  $\gamma$  bond.
25. We have not invoked the rule of Shugar and Remin – that  $H_{5''}$  is typically the upfield signal and  $H_{5'}$  is the downfield signal – as the cyclic and presumably conformationally restricted nature of the sugar-phosphate backbone in cADPR may render this observation invalid. See Remin, M.; Shugar, D. *Biochem. Biophys. Res. Comm.* **1972**, *48*, 636–642.
26. We have confirmed our “sum rule” estimate of the  $\gamma$  populations (reference 23) using the more rigorous formulae described in reference 22.
27. In the crystal structure, the N ring and A ring  $\gamma$  torsion angles were given as  $+54^\circ$  and  $+66^\circ$ , respectively, both of which would be  $\gamma^+$ . However, the *figure* in this paper appears to show both  $\gamma$ -bonds as *trans*. It is likely that the  $\gamma$ -bonds were defined using an older system where the  $\gamma$  torsion angle is defined by  $O5'-C5'-C4'-O4'$ , which would explain the  $120^\circ$  shift. The values in our discussion above have been corrected to conform with the IUPAC/JCBN guidelines.
28. Gu, Q.-M.; Sih, C.J. *J. Am. Chem. Soc.* **1994**, *116*, 7481–7486.
29. Gottlieb, H.E.; Kotlyar, V.; Nudelman, A. *J. Org. Chem.* **1997**, *62*, 7512–7515.

Received November 22, 1999

Accepted October 26, 2000





## **Request Permission or Order Reprints Instantly!**

Interested in copying and sharing this article? In most cases, U.S. Copyright Law requires that you get permission from the article's rightsholder before using copyrighted content.

All information and materials found in this article, including but not limited to text, trademarks, patents, logos, graphics and images (the "Materials"), are the copyrighted works and other forms of intellectual property of Marcel Dekker, Inc., or its licensors. All rights not expressly granted are reserved.

Get permission to lawfully reproduce and distribute the Materials or order reprints quickly and painlessly. Simply click on the "Request Permission/Reprints Here" link below and follow the instructions. Visit the [U.S. Copyright Office](#) for information on Fair Use limitations of U.S. copyright law. Please refer to The Association of American Publishers' (AAP) website for guidelines on [Fair Use in the Classroom](#).

The Materials are for your personal use only and cannot be reformatted, reposted, resold or distributed by electronic means or otherwise without permission from Marcel Dekker, Inc. Marcel Dekker, Inc. grants you the limited right to display the Materials only on your personal computer or personal wireless device, and to copy and download single copies of such Materials provided that any copyright, trademark or other notice appearing on such Materials is also retained by, displayed, copied or downloaded as part of the Materials and is not removed or obscured, and provided you do not edit, modify, alter or enhance the Materials. Please refer to our [Website User Agreement](#) for more details.

**[Order now!](#)**

Reprints of this article can also be ordered at

<http://www.dekker.com/servlet/product/DOI/101081NCN100002079>